EEG switching: three views from dynamical systems

Carlos Lourenço

[1] Faculty of Sciences of the University of Lisbon - Informatics Department,
Campo Grande, 1749-016 Lisboa - Portugal,
csl@di.fc.ul.pt,
http://www.di.fc.ul.pt/~csl
[2] Instituto de Telecomunicações - Security and Quantum Information Group,
Av. Rovisco Pais, 1, 1049-001 Lisboa - Portugal

Abstract. There is evidence that the same neural substrate may support different dynamical regimes and hence give rise to different EEG signals. However, the literature lacks successful attempts to systematically explain the different regimes —and the switching between them— within a coherent setting. We explore a mathematical model of neural tissue and call upon concepts from dynamical systems to propose a possible explanation of such processes. The model does not aim to capture a high degree of neurophysiological detail. It rather provides an opportunity to discuss the change in the signals from a dynamical perspective. Notwithstanding, realistic values are adopted for the model parameters, and the resulting EEG also shows typical frequencies in a realistic range. We identify three mechanisms accounting for change: external forcing, bifurcation, and small perturbations of a chaotic attractor.

Key words: EEG; neurodynamics; spatiotemporal dynamics; chaos.

1 Introduction

Laboratory experiments indicate that, for a given animal, a common neural substrate may display different spatiotemporal electrical activities corresponding e.g. to different behaviors or to the processing of different input patterns [1–3]. The switching between dynamical states occurs much faster than the typical time-scales of synaptic adaptation associated with learning. These findings do not contradict the well-known fact that the brain is organized in a modular fashion, with each module responsible for some type of task. However, it can be said that there continues to be a bias toward trying to identify different sub-populations that are responsible for different behaviors, rather than identifying a single population capable of a high degree of multitasking. For instance, in a study of the mouse sleep-wake behavior [4], the Authors tend to emphasize the role of the neural sub-populations that are active exclusively during either the wake stage or the sleep stages —considering also the necessary distinction between REM and non-REM sleep. These Authors attribute a minor role to the sub-populations that show activity overlapping wake and any of the sleep stages.

In the present paper we aim to unveil some of the possible dynamical mechanisms that might explain multitasking by a common neural population. This exploration is done within the framework of dynamical systems and requires a not-too-complicated model of neural tissue in order to be effective. We hope that the evidence gathered in the following numerical simulations may provide further arguments in support of the multitasking view. We have to emphasize once more that this approach does not preclude a —complementary— modular view of the brain.

A 'single-channel' model electroencephalogram (EEG) is used as a tag to confirm the switching between dynamical regimes, whenever it occurs. However, we will assess that the underlying neural dynamics is spatiotemporal. We agree with other authors in that single-channel EEG provides an incomplete account of the dynamics [5]. Yet, the type of dynamical tagging that it allows is considered sufficient for the present purposes. Furthermore, generalizing to the multi-channel case would be trivially accomplished via minor modifications of the model discussed below.

In summary, this paper tries to model those specific EEG transitions that result from some neural population changing its dynamics. It does not address the case where different neural populations are alternatingly responsible for the observed EEG.

2 Mathematical model

We adopt a 'minimal' model in what concerns biological realism. We wish to retain the main properties of neurons which may influence the dynamical behavior both at the single cell and at the network level. At least at an abstract level, these dynamics should be comparable to those of biological neurons. On the other hand, we assume that the intricacies of multi-compartment neurons and different types of real neuron connections are not necessary at this level of abstraction, as they should not invalidate the main dynamical mechanisms that we wish to unveil. When considering the full network, a range of diverse spatiotemporal dynamical regimes is our target for study. Some of these regimes may be denoted as complex, or even chaotic.

Neural oscillations in electrical activity, which are ultimately responsible for the observed EEG, result from an interplay between neural excitation and inhibition. Hence we consider two different neural populations, respectively, of excitatory and inhibitory neurons. Our model is based on an original proposal of Kaczmarek to explain neural firing patterns during epileptic seizures [6], but we believe it is general enough to be of use in modeling different brain states, notably in the cases of comparing different awareness states or states supporting cognitive actions. See also the model developments in [7]. The model of the individual cell can be described as a leaky integrator. Passive as well as active membrane properties are incorporated, but neural connectivity is simplified to the point where only first-neighbor coupling is considered. This elimination of distant connections provides a means to study those particular dynamical pro-

cesses where the spatial dimension plays a crucial role, such as the development of certain complex spatiotemporal dynamics. This includes wave propagation and related phenomena. Biological plausibility is enhanced by a highly nonlinear neural coupling, as well as the consideration of delays in signal transmission between neurons. These model features account for the nonlinear transformation between membrane potential and firing rate, as well as for the several synaptic and axonal processes contributing to a non-instantaneous information propagation. Realistic values are chosen for the parameters wherever possible.

2.1 A model of neural tissue

For lack of space in the present publication, we refer the reader to the detailed derivation of our model in [8]. Here we summarize only the main features.

The instantaneous values of each neuron's membrane potential are taken as network state variables. Since delays are considered, the dynamical evolution also depends on past membrane potential values; hence the latter also define the state vector, which is thus infinite-dimensional. The neurons communicate their state to each other trough a firing rate code. Therefore, there is no explicit spiking in the model. In spite of this, it can be noted that a stationary state corresponds to the firing of action potentials with a frequency constant in time. This frequency can be close to zero, or have some finite value. An oscillatory state, on the other hand, implies a time-modulation of the firing frequency.

The derivation starts with a resistive-capacitive equation for the electrical equivalent of each neuron's membrane potential, and ends up with a coupled set of delay differential equations for the neural population. The network comprises $N_{\rm ex}$ excitatory neurons X_i, and $N_{\rm in}$ inhibitory neurons Y_j. Their dynamics is given by $\mathrm{d}X_i/\mathrm{d}t = -\gamma(X_i - V_L) - (X_i - E_1)\sum_{k\neq i}\omega_{ik}^{(1)}\,F_X[X_k(t-\tau_{ik})] - (X_i - E_2)\sum_{l\neq i}\omega_{il}^{(2)}\,F_Y[Y_l(t-\tau_{il})]$ and $\mathrm{d}Y_j/\mathrm{d}t = -\gamma(Y_j - V_L) - (Y_j - E_1)\sum_{k\neq j}\omega_{jk}^{(3)}\,F_X[X_k(t-\tau_{jk})]$, respectively, where $i,k = 1,\ldots,N_{\rm ex}$ and $j,l = 1,\ldots,N_{\rm in}$. The inverse of the membrane's time-constant takes the value $\gamma = 0.25\ \mathrm{msec}^{-1}$. The propagation delay τ_{ik} between neurons k and i would generally depend on the distance between the two neurons. Since we consider only first-neighbor connections, a fixed value $\tau = 1.8$ msec is adopted. Other parameter values are $V_L = -60$ mV, $E_1 = 50$ mV, and $E_2 = -80$ mV, these being the different equilibrium potentials. The sigmoidal transfer function is defined by $F(V) = 1/(1+e^{-\alpha(V-V_c)})$, with parameter values V_c=−25 mV, $\alpha_X = 0.09\ \mathrm{mV}^{-1}$, and $\alpha_Y = 0.2\ \mathrm{mV}^{-1}$. Notice the different α slopes for excitatory and inhibitory neurons, respectively. The synaptic weights $\omega_{ik}^{(1)}$, $\omega_{il}^{(2)}$, and $\omega_{jk}^{(3)}$ refer, respectively, to excitatory-to-excitatory, inhibitory-to-excitatory, and excitatory-to-inhibitory connections. No inhibitory-to-inhibitory connections are considered. We study a spatially homogeneous network, where all synaptic weights of the same type have the same value. Furthermore, the ω values are constant in time, thus no adaptation or learning takes place. However, we will consider deviations from a set of adopted nominal ω values, for instance in a bifurcation setting. The

weights of types (1) and (3) are fixed at $\omega^{(1)} = 3.15$ and $\omega^{(3)} = 2.5$ respectively. Parameter $\omega^{(2)}$ can have different values; a reference value is $\omega^{(2)} = 1.68$.

In the isolated model neuron, the response of the membrane to some finite-duration perturbation from the resting state would be a simple relaxation. However, through the coupling of the neurons, new dynamical regimes can be observed depending on details of the coupling and on the initial conditions of the network. One can observe multiple steady states, including global quiescence and global saturation, as well as a variety of oscillatory regimes for the electrical activity of the neurons. A form of spatiotemporal chaos is one of the observed complex regimes, as discussed in more detail in [8].

Different connectivity configurations have been explored for this general neural arrangement, including the case of bi-dimensional networks with many excitatory and inhibitory neurons. However, here we consider only a 1-D spatial arrangement. The network features 16 neurons, equally divided into an excitatory and an inhibitory population. Hence $N_{\text{ex}} = N_{\text{in}} = 8$. The network topology is depicted in Fig. 1.

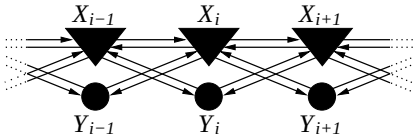

Fig. 1. Neural network where the dynamics takes place. Excitatory neurons and inhibitory neurons are represented as triangles and circles, respectively. Connections $X_i \to X_{i\pm1}$ and $X_i \to Y_{i\pm1}$ are excitatory, whereas connections $Y_i \to X_{i\pm1}$ are inhibitory.

The previous dynamical equations are simplified such that only first-neighbor connections are kept. The boundary conditions are of the zero-flux type.

2.2 A model of EEG

Our model EEG measurement is best regarded as a signal denoting a field potential. We follow a few basic assumptions in defining this potential, or the resulting EEG. We avoid the complicated practical issues that involve the actual measurement of the EEG in a laboratory. The EEG results from extracellular current flow associated with integrated synaptic potentials in activated neurons. The intracellular potentials are not directly accessible via EEG measurements. Pyramidal cells, which are excitatory, are the major source of the EEG. They are oriented parallel to one another, and most of their dendrites are oriented perpendicularly to the surface of the cortex [9]. Therefore, current flows are mostly oriented in the same fashion. In contrast, other types of cells do not share any common orientation and thus their individual contributions do not sum up.

In the context of our model, the synaptic current sources are those corresponding to excitatory neurons X_i at spatial locations $\mathbf{r}_i$ and are given by

$I_{\rm m}(\mathbf{r}_i,t) = C_{\rm m}\Big[-(X_i-E_1)\sum_{j=i\pm1}\omega_{ji}^{(1)}\,F_X[X_j(t-\tau_{ji})]$
$-(X_i-E_2)\sum_{j=i\pm1}\omega_{ji}^{(2)}\,F_Y[Y_j(t-\tau_{ji})]\Big]$, where $i=1,\ldots,N_{\rm ex}$ and $C_{\rm m}$ is the membrane capacitance. The field potential at a point $\mathbf{r}_{\rm e}$ of the extracellular space incorporates the contributions from all excitatory neurons: $V(\mathbf{r}_{\rm e},t) = (1/(4\pi\sigma))\sum_i \left(I_m(\mathbf{r}_i,t)/|\mathbf{r}_i-\mathbf{r}_{\rm e}|\right)$, where σ represents the electrical conductivity of the extracellular medium. The measurement of the model EEG is performed according to the scheme of Fig. 2.

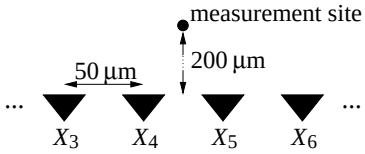

Fig. 2. Relative positions of the current sources and of the EEG voltage measurement site.

3 Change in the dynamics and the resulting EEG

We take, as the network's typical dynamical state, one where spatiotemporal oscillations of the membrane potential are observed. This is the case for the parameter region considered [8]. Traveling waves are mathematically possible. However, due to the relation between wavelength, system size, and boundary conditions, the waves are in this case geometrically constrained. Details of the full dynamics are out of the scope of this paper. We focus on the fact that the underlying neural network may undergo specific changes in its dynamical state through any of the mechanisms identified in the next sections. The EEG follows these changes and may be used as a tag thereof.

3.1 Change in response to external forcing

Let us take $\omega^{(2)} = 1.68$ and all other parameters as indicated in Section 2.1. The dynamics of the unperturbed network is spatiotemporal. This means that, at any time, different neurons generally display different values of the membrane potential. However, the dynamics of the full network is periodic as revealed by a EEG signal which has a period $T = 25.62$ msec.

From this reference dynamical condition, we perturb a fraction of the neurons with an external stimulus of finite magnitude. Namely, we perturb excitatory neurons X_1 through X_4 with a simulated injected electric current. In the mathematical model, this is actually equivalent to momentarily shifting the value of the resting potential V_L. The external perturbation signal could also have its own intricate dynamics, and the network's response to such a signal might be viewed as an analog computation performed over an input pattern. Such ideas are discussed e.g. in [10], but they are not the focus of the present paper.

Here we use a static perturbation with a simple form. Having allowed the network to evolve autonomously for some time, we choose a certain instant to

activate the perturbation, and mark this instant as $t = 0$. The perturbation then remains activated for the duration of the numerical experiment. The perturbation consists in shifting V_L by $+5$ mV for neurons X_1 through X_4.

As a result of the perturbation, the dynamics remains periodic but the EEG period changes to $T = 50.13$ msec. Figure 3 displays the EEG signal, respectively, without and with the described perturbation activated.

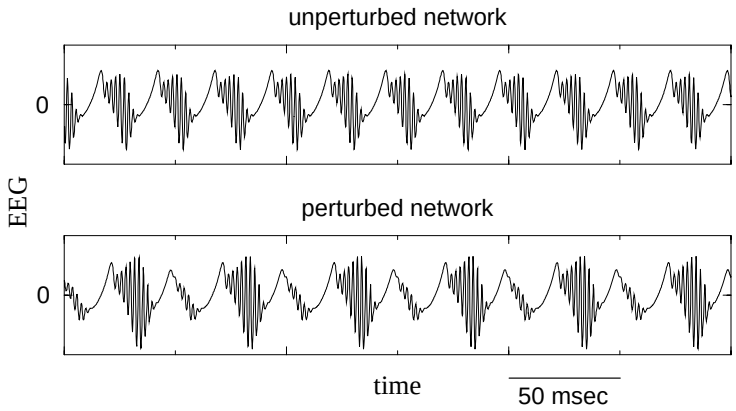

Fig. 3. Comparison between the EEG measured from a network which suffers a finite-size perturbation, and the EEG from an unperturbed network. An arbitrary 300 msec interval is shown. The transient dynamics right after the onset of perturbation is not depicted since we choose to make it occur prior to the plotted interval. See text for details of the perturbation. $\omega^{(2)} = 1.68$ and the remaining parameters are as indicated in Section 2.1.

3.2 Change by following a bifurcation path

Let us now consider that no external perturbation is present. Instead, an internal system parameter is available for change. We select the value of the synaptic weight $\omega^{(2)}$ to be varied.

We take the values $\omega^{(2)} = 3.00$ and $\omega^{(2)} = 1.68$, one at a time, and inspect the dynamics that occurs for each of these values. Again, all other parameters are as indicated in Section 2.1. Also in this case, the EEG is used as a probe of the dynamics. Lowering $\omega^{(2)}$ from 3.00 to 1.68 is actually just walking a small path in the complex parameter space of the neural network. However, it is enough to elicit a visible transition in the dynamics. This parameter variation is part of a larger bifurcation path. A larger $\omega^{(2)}$ range than the one shown here would produce a full period-doubling bifurcation scenario [8]. Figure 4 displays the EEG signal for $\omega^{(2)} = 3.00$ and $\omega^{(2)} = 1.68$, respectively. The EEG period is $T = 17.28$ msec when the inhibition is higher and $T = 25.62$ msec when the inhibition is lower. This numerical experiment, if taken isolatedly and resorting

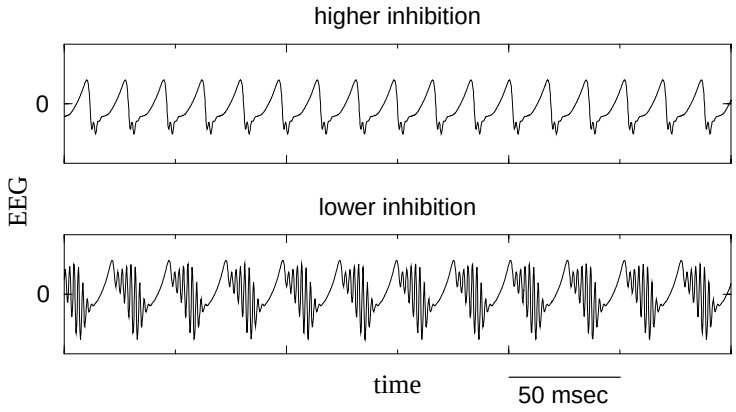

Fig. 4. Comparison of the EEG measured for two different values of synaptic inhibition in the network. As in Fig. 3, an arbitrary 300 msec interval is shown. The vertical scale is also the same as in Fig. 3. The higher inhibition corresponds to $\omega^{(2)} = 3.00$ and the lower inhibition to $\omega^{(2)} = 1.68$. The remaining parameters are as indicated in Section 2.1.

only to the EEG signal, would not suffice to suggest the occurrence of period-doubling bifurcations.

3.3 Switching within a chaotic attractor

We now take $\omega^{(2)} = 1.64$ and let all other parameters have the usual values as indicated in Section 2.1. Finite perturbation of the neural system is excluded, be it through some external influence or through parameter change as in the bifurcation scenario. However, 'infinitesimal' perturbations are allowed. The latter can consist in occasional minute changes to system variables, or in occasional minute shifts in a system parameter. Any of the the latter types of perturbations are to be distinguished from the finite perturbations of sections 3.1 and 3.2, since they correspond to different orders of magnitude.

As reported in [8], for these parameter values the system displays a form of low-dimensional spatiotemporal chaos. The dynamics is not periodic, but moderate coherence is observed in the neurons' activities. The change in electrical activity across the network tends to follow a wavy pattern. This is quite far from, say, a regime of fully developed turbulence. Furthermore, the dynamics is coherent enough that it can be switched in a controlled way via an infinitesimal perturbation such as the ones referred above. For this to be possible, two essential properties of chaos come into play: 1) the chaotic dynamics is very flexible and extremely sensitive to small perturbations; 2) under appropriate conditions (verified here), the chaotic attractor contains an infinite number of unstable periodic orbits (UPOs). Infinitesimal perturbations, if adequately tuned, may switch the chaotic dynamics into one of those UPOs, or switch the dynamics between different UPOs. These transitions can be very fast.

In [11, 8, 10], it is argued that this mechanism may place the chaotic system in an appropriate state for some type of information processing. This UPO selection need not last longer than the time required for a particular computational task. We do not intend to further re-state those ideas here, but rather put forth the EEG signal as a side-effect of, or a tag for, some of those UPOs that can be selected in practice. Since the UPOs are unstable by nature, they cannot be sustained in time unless some control mechanism performs occasional infinitesimal perturbations obeying a so-called control algorithm. This too is out of the scope of the present paper.

Figure 5 allows to compare the EEG signal, respectively, for the unperturbed

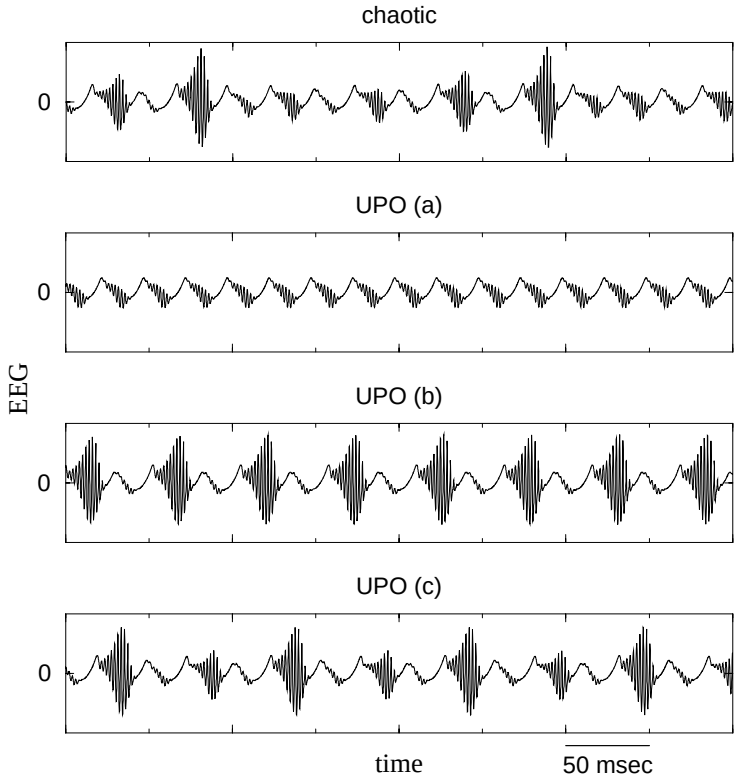

Fig. 5. With $\omega^{(2)} = 1.64$ and the remaining parameters as indicated in Section 2.1, the unperturbed network displays a chaotic regime. Its corresponding EEG is show at the top of the figure. Via infinitesimal perturbations, the dynamics can be switched into a number of different UPOs. In contrast to the broadband frequency spectrum of chaos, the UPOs possess well-defined natural frequencies. Their respective values are: **(a):** 39.79 Hz; **(b):** 18.96 Hz; **(c):** 9.61 Hz. Notice the different time-scale as compared to the one in Figs. 3 and 4. In the present figure an arbitrary 400 msec interval is shown. Also, the vertical scale is compressed by a factor of 1.875 with respect to the one in Figs. 3 and 4.

chaotic attractor, and for three particular UPOs that are embedded in the chaotic attractor. Thus a multitude of possible dynamical regimes coexist within the chaotic attractor. They are in principle accessible through tiny perturbations of the attractor. The EEG of the dynamical regimes illustrated in Fig. 5 turns out to possess natural frequencies in a realistic range. It should be noted that these EEG signals are all produced by the same neural population, which is (infinitesimally) perturbed in different manners starting from a common chaotic regime.

4 Discussion

We identified three different mechanisms that may account for changes in the spatiotemporal neural dynamics. These changes imply transitions in the EEG, which is a scalar observable, or tag.

The first type of change, through external forcing, requires that a finite-size perturbation reach the neurons. 'External' here means external to the neural population we are modeling, not necessarily external to the organism. As it comes, a primary cue, eventually one with limited time-span, may be used by some distinct neural population for it to enter a state in which it provides afferent input to our particular neural population —the one that does the dynamical multitasking.

The second type of change depends on an internal parameter being available for change. If the parameter range so allows, bifurcations may be observed. In the latter case, the transitions in the dynamics will be clearly noticeable. However, an adequate parameter is not always available, or the time-scales for the parameter change might be slower than required. Furthermore, such type of change might be metabolically costly. Notwithstanding, certain neuromodulators might play a role in these processes. Acetylcholine, for instance, has a confirmed action in the modulation of attentional processes. Interestingly, attentional processes also provide distinct EEG frequencies directly associated with behavior. We also note that the variation of certain internal parameters may have an effect equivalent to that of an external forcing.

The third type of dynamical switching is the fastest and most flexible, since the dynamics is not constrained to some limit-cycle behavior. Rather, the spatiotemporal chaotic regime allows that multiple behaviors be simultaneously available in the form of UPOs. Yet, this generally requires that an adequate mechanism be available to select the most favorable UPO for a given task.

Of course, a combination of more than one of the scenarios is possible. For instance, in separate articles we discuss the consequences of perturbing a chaotic regime with a finite-size external perturbation [10, 11], apart from the infinitesimal perturbations that provide UPO switching. This is done from a computational standpoint, and the aim is to assess the pattern processing capabilities of chaotic neural networks.

The model that we discussed in this article supports all three scenarios in a homogeneous way. The chaotic 'mode' could be the most promising. However, the dispute over the very existence of low-dimensional chaos in the brain has not been settled even if more than 20 years have passed since the seminal claims [12, 13]. Here we keep an open perspective, and try to determine what actual use chaos may have for any system —natural or artificial— where it may occur [11].

Our last comment is on the particular set of EEG frequencies that are somewhat 'hidden' in our chaotic model, and that can be elicited trough minute perturbations. The 9.61 Hz falls into the alpha range, whereas the 39.79 Hz is in the gamma range. The latter range contains the famous "40 Hz" oscillations. These frequencies have been obtained without any purposeful tuning of the system's parameters. They can be regarded as an emergent phenomenon.

Acknowledgments. The author acknowledges the partial support of Fundação para a Ciência e a Tecnologia and EU FEDER via Instituto de Telecomunicações and via the project PDCT/MAT/57976/2004.

References

1. Wu, J.-Y, Cohen, L., Falk, C.: Neuronal activity during different behaviors in *Aplysia*: A distributed organization? Science **263** (1994) 820–823
2. Freeman, W.: The physiology of perception. Scientific American **264** (1991) 78–85
3. Freeman, W.: Chaos in the CNS: Theory and practice. In Ventriglia, F. (ed.): Neural Modeling and Neural Networks. Pergamon Press, New York (1994) 185–216
4. Diniz Behn, C., Brown, E., Scammell, T., Kopell, N.: Mathematical model of network dynamics governing mouse sleep-wake behavior. Journal of Neurophysiology **97** (2007) 3828–3840
5. Lachaux, J.-P, Pezard, L., Garnero, L., Pelte, C., Renault, B., Varela, F., Martinerie, J.: Spatial extension of brain activity fools the single-channel reconstruction of EEG dynamics. Human Brain Mapping **5** (1997) 26–47
6. Kaczmarek, L.: A model of cell firing patterns during epileptic seizures. Biological Cybernetics **22** (1976) 229–234
7. Destexhe, A.: Ph.D. Dissertation, Université Libre de Bruxelles, March 1992.
8. Lourenço, C.: Dynamical computation reservoir emerging within a biological model network. Neurocomputing **70** (2007) 1177–1185
9. Kandel, E., Schwartz, J., Jessel, T. (eds.): Principles of Neural Science, 3rd Edition. Prentice-Hall, Englewood Cliffs, New Jersey (1991)
10. Lourenço, C.: Structured reservoir computing with spatiotemporal chaotic attractors. In Verleysen, M. (ed.): 15th European Symposium on Artificial Neural Networks (ESANN 2007), April 25-27. d-side publications (2007) 501–506
11. Lourenço, C.: Attention-locked computation with chaotic neural nets. International Journal of Bifurcation and Chaos **14** (2004) 737–760.
12. Babloyantz, A., Salazar, J., Nicolis, C.: Evidence of chaotic dynamics of brain activity during the sleep cycle. Physics Letters A **111** (1985) 152–156
13. Rapp, P., Zimmerman, I., Albano, A., de Guzman, G., Greenbaun, N.: Dynamics of spontaneous neural activity in the simian motor cortex: The dimension of chaotic neurons. Physics Letters A **110** (1985) 335–338